

# Electron-neutrino scattering off nuclei from two different theoretical perspectives

M. Martini<sup>1,2</sup>, N. Jachowicz<sup>1</sup>, M. Ericson<sup>3,4</sup>, V. Pandey<sup>1</sup>, T. Van Cuyck<sup>1</sup>, N. Van Dessel<sup>1</sup>

<sup>1</sup>*Department of Physics and Astronomy, Ghent University,  
Proeftuinstraat 86, B-9000 Gent, Belgium*

<sup>2</sup>*ESNT, CEA-Saclay, IRFU, Service de Physique Nucléaire,  
F-91191 Gif-sur-Yvette Cedex, France*

<sup>3</sup>*Université de Lyon, Univ. Lyon 1, CNRS/IN2P3,  
IPN Lyon, F-69622 Villeurbanne Cedex, France and*

<sup>4</sup>*Physics Department, Theory Unit,  
CERN, CH-1211 Geneva, Switzerland*

## Abstract

We analyze charged-current electron-neutrino cross sections on Carbon. We consider two different theoretical approaches, on one hand the Continuum Random Phase Approximation (CRPA) which allows a description of giant resonances and quasielastic excitations, on the other hand the RPA-based calculations which are able to describe multinucleon emission and coherent and incoherent pion production as well as quasielastic excitations. We compare the two approaches in the genuine quasielastic channel, and find a satisfactory agreement between them at large energies while at low energies the collective giant resonances show up only in the CRPA approach. We also compare electron-neutrino cross sections with the corresponding muon-neutrino ones in order to investigate the impact of the different charged-lepton masses. Finally, restricting to the RPA-based approach we compare the sum of quasielastic, multinucleon emission, coherent and incoherent one-pion production cross sections (folded with the electron-neutrino T2K flux) with the charged-current inclusive electron-neutrino differential cross sections on Carbon measured by T2K. We find a good agreement with the data. The multinucleon component is needed in order to reproduce the T2K electron-neutrino inclusive cross sections.

PACS numbers: 25.30.Pt, 13.15.+g, 24.10.Cn

## I. INTRODUCTION

Recent years have seen an accumulation of data on muon-neutrino cross sections on nuclei at intermediate energies [1–19]. These measurements have revealed interesting features in different reaction channels. For example, the charged-current quasielastic (CCQE) measurement performed by MiniBooNE [1] has attracted a lot of attention due to its unexpected behavior, reproducible with an unphysical value of the axial mass. This axial mass anomaly is now explained by the inclusion of events in which several nucleons are ejected in the CCQE cross section [20–33]. In the one-pion production channel some questions are still open. For instance, various theoretical models [34, 35] cannot simultaneously reproduce the MiniBooNE [2, 5] and the MINERvA [15] results.

The wealth of experimental and theoretical results on muon-neutrino cross sections contrasts with the few published results on electron-neutrino cross sections. After the inclusive  $\nu_e$  CC total cross sections measured by the Gargamelle bubble chamber in 1978 [36], the first measurement of inclusive  $\nu_e$  CC differential cross sections on Carbon was performed by T2K [37]. Recently the measurement performed by MINERvA of quasielastic and quasielastic-like differential cross sections on Carbon also appeared [38]. A precise knowledge of  $\nu_\mu$  and  $\nu_e$  cross sections is important in connection to the  $\nu_\mu \rightarrow \nu_e$  oscillation experiments which aim at the determination of the neutrino mass hierarchy and the search for CP violation in the lepton sector. A theoretical comparison of the  $\nu_\mu$  and  $\nu_e$  cross sections was performed by Day and McFarland [39] who analyzed the influence of the final lepton-mass difference on the cross sections as a function of the neutrino energy and of  $Q^2$ . Here we study these differences focusing on the  $\nu_\mu$  and  $\nu_e$  differential cross sections. In a first part we consider the electron-neutrino cross sections on Carbon using two different theoretical models. The first one is the one of Martini *et al.* [20] which is based on nuclear response functions, treated in the random phase approximation (RPA) on top of a local relativistic Fermi gas (LRFG) calculation. It includes the quasielastic cross section, multinucleon emission and coherent and incoherent single pion production. The second model is the one of Jachowicz *et al.* [40] which is based on the continuum random phase approximation (CRPA) on top of Hartree-Fock (HF) calculations. It was originally developed to study electroweak reactions in the giant resonance region and then extended by Pandey *et al.* [41, 42] to the quasielastic regime. The common channel where the two approaches can be compared is hence the

quasielastic one. After a brief description of the two theoretical models, we confront their results in the quasielastic channel, first for fixed kinematics, then folding them with the T2K and the MiniBooNE  $\nu_e$  fluxes. We also illustrate in both models the differences between  $\nu_\mu$  and  $\nu_e$  cross sections. Finally, we compare the predictions in the approach of Martini *et al.*, with the inclusive  $\nu_e$  CC differential cross sections on Carbon recently measured by T2K [37]. We postpone the comparison with the very recent MINERvA results [38] to a future paper.

## II. THEORETICAL MODELS

We summarize here the basic ingredients of the two models. Both approaches calculate the polarization propagator  $\Pi$  in the random phase approximation (RPA) which allows the inclusion of long-range nucleon-nucleon correlations. This amounts to solving integral equations which have the generic form

$$\Pi = \Pi^0 + \Pi^0 V \Pi, \quad (1)$$

where  $\Pi^0$  is the bare polarization propagator and  $V$  denotes the effective particle-hole interaction. However, the bare polarization propagator and the residual interaction differ in the two approaches. For Martini *et al.* [20] the bare polarization propagator is evaluated in momentum space. In a finite system it is non-diagonal and writes  $\Pi^0(\omega, \mathbf{q}, \mathbf{q}')$ . In order to account for the finite-size effects, it is evaluated in a semi-classical approximation [43, 44] where it can be cast in the form

$$\Pi^0(\omega, \mathbf{q}, \mathbf{q}') = \int d\mathbf{r} e^{-i(\mathbf{q}-\mathbf{q}')\cdot\mathbf{r}} \Pi^0\left(\omega, \frac{\mathbf{q}+\mathbf{q}'}{2}, \mathbf{r}\right). \quad (2)$$

To obtain this quantity, a local density approximation is used which relates the final result to the relativistic Fermi gas polarization propagator according to

$$\Pi^0\left(\omega, \frac{\mathbf{q}+\mathbf{q}'}{2}, \mathbf{r}\right) = \Pi_{k_F(r)}^0\left(\omega, \frac{\mathbf{q}+\mathbf{q}'}{2}\right). \quad (3)$$

The local Fermi momentum  $k_F(r)$  is related to the experimental nuclear density through :  $k_F(r) = (3/2\pi^2 \rho(r))^{1/3}$ . The density profiles of  $^{12}\text{C}$  are taken from the Sum-of-Gaussians nuclear charge density distribution parameters according to Ref. [45]. In the approach of Jachowicz *et al.* [40], the starting point is the continuum Hartree-Fock model which

evaluates the bound and the continuum single-nucleon wave functions through the solution of the Schrödinger equation with a mean field potential. The bare polarization propagator, in this case the HF one, is then calculated in coordinate space.

The particle-hole residual interaction differs as well in the two approaches. In the Martini *et al.* one, a parameterization in terms of pion exchange, rho exchange and contact Landau-Migdal parameters is used while in the Jachowicz *et al.* model, the same Skyrme-type interaction which enters in the mean field calculation is employed to generate the continuum RPA (CRPA) solution. In this way, this calculation becomes self-consistent with respect to the interaction used. In Ref. [42] this residual Skyrme-type interaction is multiplied by a dipole form factor which controls the influence of the residual interaction at high  $Q^2$  values.

Concerning the RPA differences, an important point should be mentioned. The possibility of  $\Delta$  excitation is included explicitly in the case of Martini *et al.* This is reflected in the appearance, in certain kinematical regions, of a sizeable quenching of the RPA results, due to the mixing of nucleon-hole states with  $\Delta$ -hole ones, the Ericson-Ericson–Lorentz-Lorenz (EELL) effect [47]. This quenching has been introduced and established in pion scattering [47]. It has been discussed also in relation with electron [46] and neutrino [20, 25, 48] scattering.

### III. COMPARISON BETWEEN THEORETICAL CALCULATIONS

#### A. LRFG+RPA *vs* HF+CRPA

In this Subsection, we compare the theoretical results in the one nucleon-one hole sector obtained in the two different approaches. We consider the  $\nu_e$ - $^{12}\text{C}$  double differential cross sections for different values of the neutrino energy and lepton scattering angle. These cross sections are purely theoretical quantities since the experimental ones depend on the neutrino fluxes and hence are specific for each experiment. In Fig.1 we display the results of the two approaches by switching on and off the residual particle-hole interaction. We keep the same notations as in the previous papers of the groups. Namely we call “bare-LRFG” the results of Martini *et al.* when the particle-hole interaction is switched off (these are relativistic Fermi gas results in the local density approximation) and “RPA” the results obtained by switching on the particle-hole interaction. The corresponding results in the case of Jachowicz *et al.* are

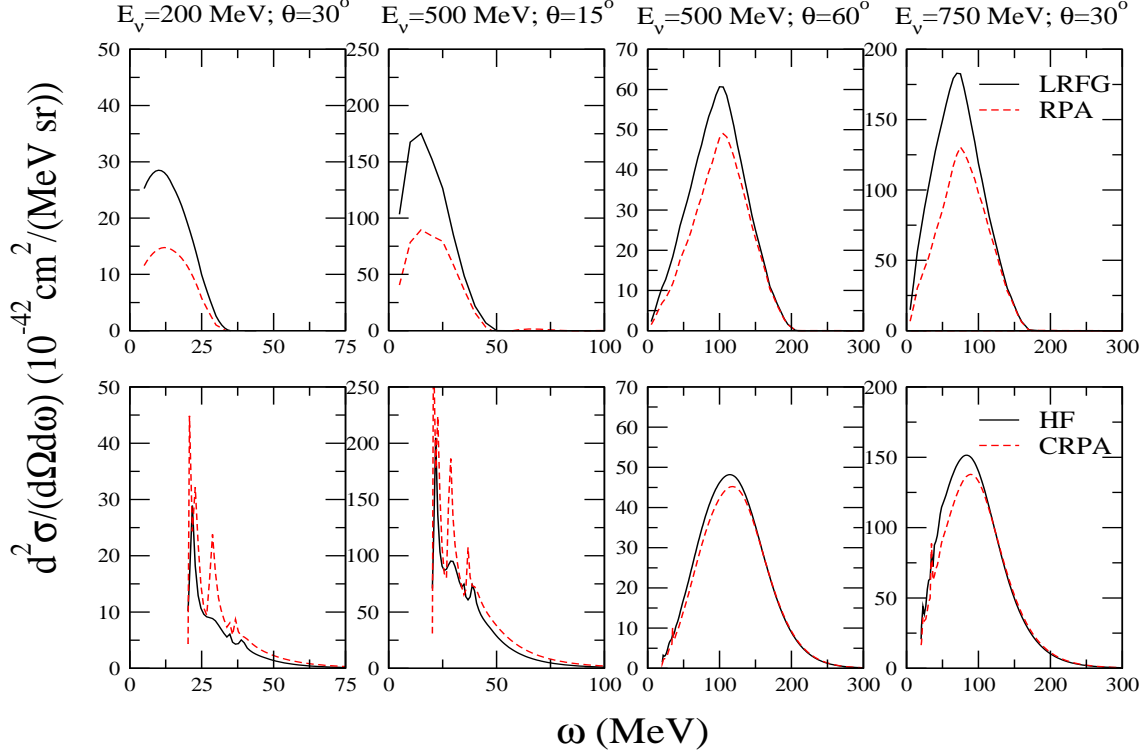


FIG. 1: (Color online) Electron-neutrino CC double differential cross section on Carbon for fixed values of scattering angles and incident neutrino energies as a function of the energy transferred to the nucleus. In the upper (lower) panels the results obtained in the bare-LRFG (HF) and RPA (CRPA) approaches are displayed. Only genuine quasielastic and giant resonance excitations (given by the CRPA) are considered.

called “HF” and “CRPA”. Some important differences between the two approaches appear. The most striking feature is the appearance of giant resonance peaks in the CRPA results of Jachowicz *et al.* They vanish for large neutrino energy or larger scattering angle. The second comment concerns the threshold energy in the HF+CRPA approach, about  $\simeq 18$  MeV, which reflects the nucleon separation energy, ignored in the semi-classical approximation of Martini *et al.* The HF+CRPA results also display the shell structure, which is not present in the semiclassical description. It disappears at large angles or energies, where the two approaches become more similar. However, when compared to the semiclassical LRFG results, in the mean field HF case the quasielastic peak is somewhat quenched and the high transferred-energy tail is more important. This is a consequence of the non-locality of the mean field which quenches and hardens the responses.

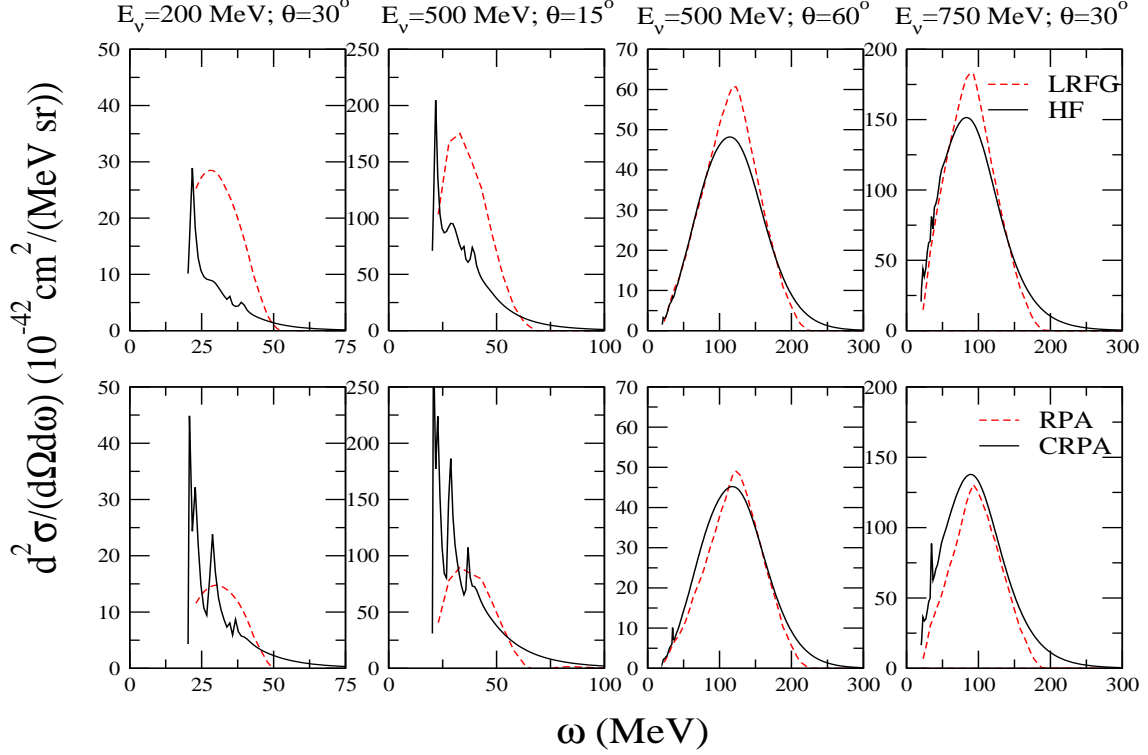


FIG. 2: (Color online) Electron-neutrino CC double differential cross section on Carbon for fixed values of scattering angles and incident neutrino energies as a function of the energy transferred to the nucleus. In the upper (lower) panels the results obtained in the bare-LRFG (RPA) and HF (CRPA) approaches are displayed. Only genuine quasielastic and giant resonances excitations (given by the CRPA) are considered. Continuous lines: HF and CRPA results; dashed lines: LRFG and RPA results shifted by 18 MeV.

Turning to RPA effects, the important difference is the large RPA quenching in the Martini *et al.* approach, due to the mixing with  $\Delta$ -hole states that we have commented before, not explicitly present in the CRPA results of Jachowicz *et al.*

In order to better illustrate the comparison between the two approaches, we show in Fig. 2 the LRFG and RPA results shifted by 18 MeV, an average value of the separation energy, and we compare them with the HF and CRPA results respectively. For the structureless part of the cross sections, *i.e.* for the kinematical conditions dominated by the quasielastic excitations (*e.g.*  $\theta = 60^\circ$  and  $E_{\nu_e} = 500$  MeV or  $\theta = 30^\circ$  and  $E_{\nu_e} = 750$  MeV), the two approaches are essentially in agreement. Furthermore the HF and CRPA cross sections are characterized by stronger tails at high transferred energies. In the low-energy part, the

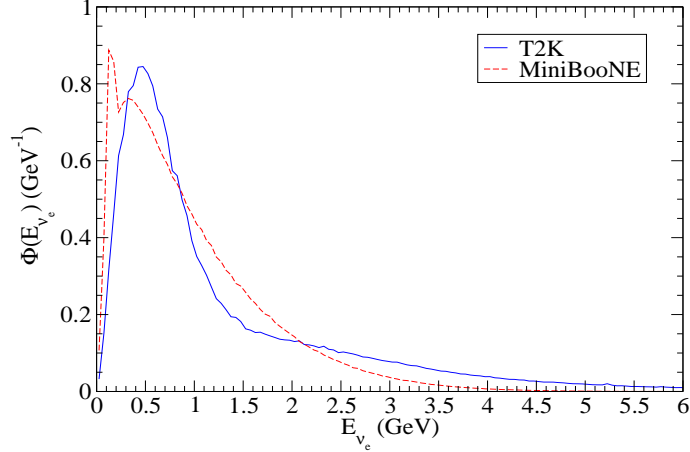


FIG. 3: (Color online) Normalized electron-neutrino T2K [49] and MiniBooNE [50] fluxes.

RPA results (which do not show giant resonance peaks) represent the average of the CRPA calculations relatively well.

Turning to the flux folded cross sections we consider the T2K [49] and MiniBooNE [50]  $\nu_e$  normalized fluxes, which are shown in Fig. 3. We discuss single-differential cross sections,  $\frac{d\sigma}{dp_e}$  and  $\frac{d\sigma}{d\cos\theta_e}$ , their theoretical evaluation is displayed in Fig. 4. One observes that the giant resonance effects are no longer apparent and that in general the differences between HF and CRPA calculations are largely washed out by the flux folding, except maybe for very forward scattering. Moreover in the case of MiniBooNE fluxes the HF or CRPA results are very similar to the LRFG ones while the RPA curves, which are somewhat below, display the usual EELL quenching. In the T2K case instead some small differences appear: the HF and CRPA results are above the corresponding LRFG cross section. This difference, which did not show with the MiniBooNE flux, is the effect of the larger T2K high energy tail. The differences between the two different theoretical models are weighted in different ways by the different flux profiles. But apart from the RPA quenching the differences are small.

### B. $\nu_e$ vs $\nu_\mu$ cross sections

After the discussion of the differences between the two approaches for the  $\nu_e$  case, we turn to a comparison between the charged current  $\nu_e$  and  $\nu_\mu$  cross sections. In order to show some theoretical results in touch with the experimental situation, we present in Fig. 5 the double differential cross sections in the different channels for fixed values of the scattering

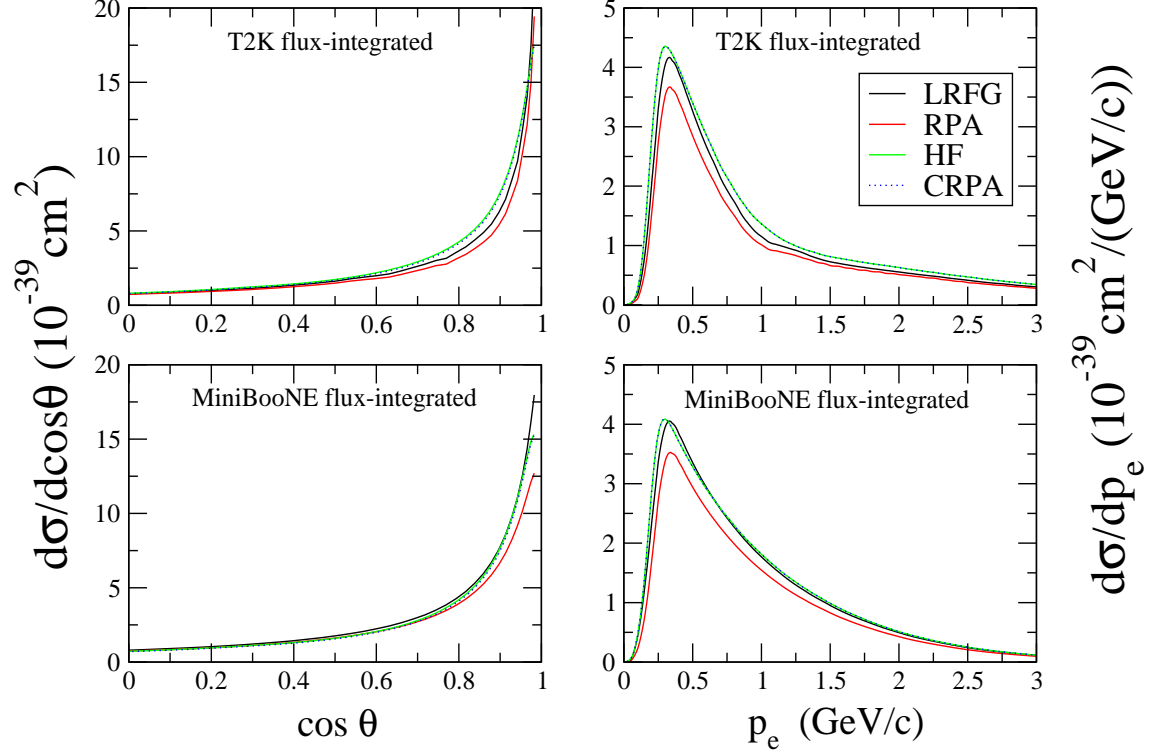


FIG. 4: (Color online) Electron-neutrino T2K and MiniBooNE flux-folded CC single differential cross sections on Carbon per nucleon.

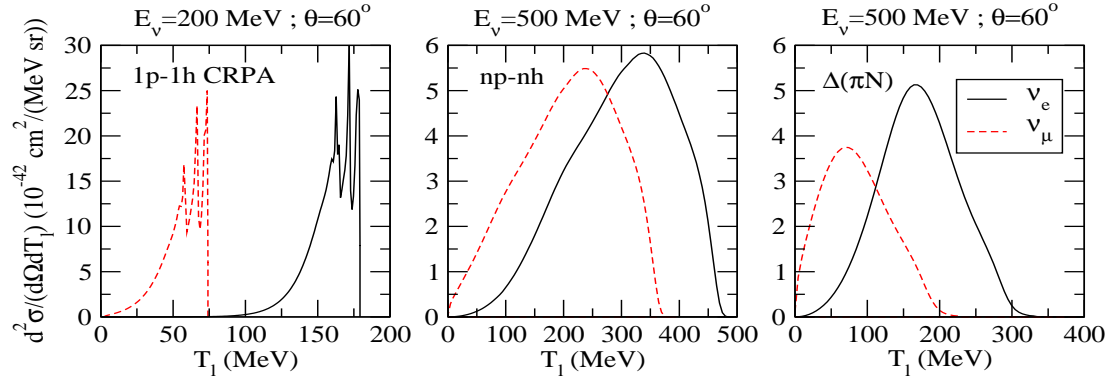


FIG. 5: (Color online) Electron- and muon-neutrino CC double differential cross section on Carbon for fixed values of scattering angles and incident neutrino energies as a function of the charged lepton kinetic energy. Left panel: 1p-1h excitations in CRPA; middle panel: np-nh excitations; right panel: incoherent one pion production contribution.



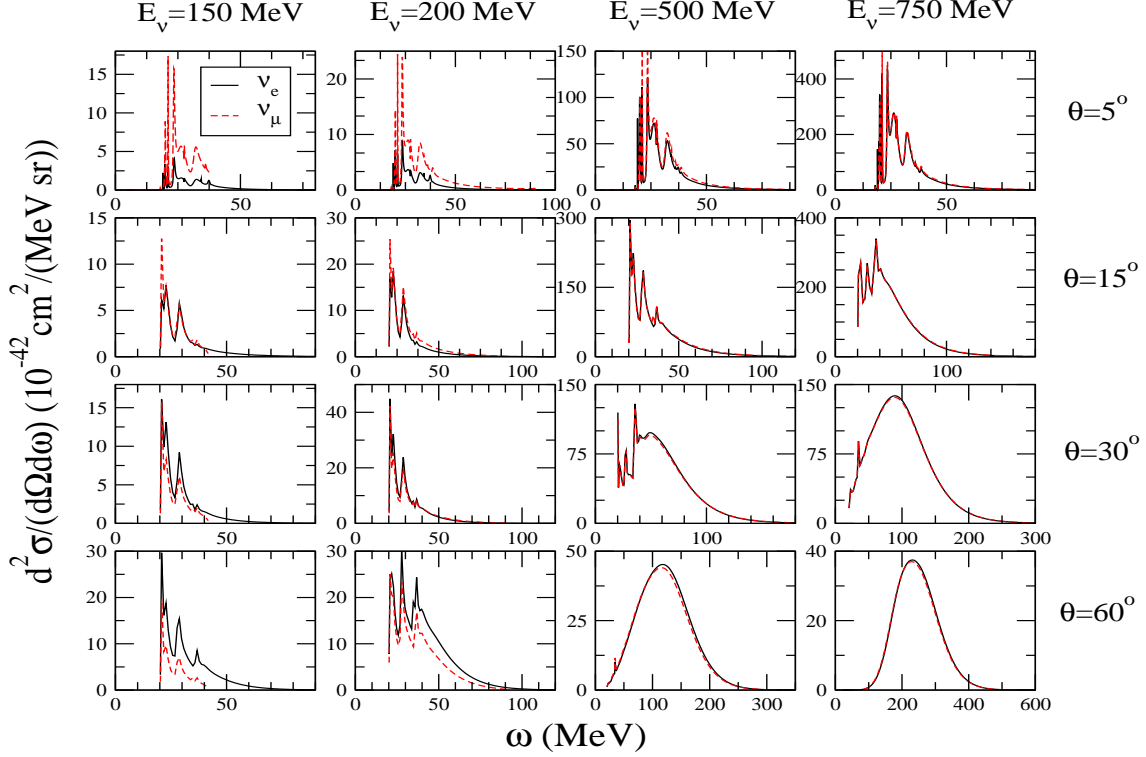


FIG. 6: (Color online) Electron- and muon-neutrino CC double differential cross section on Carbon calculated in the CRPA approach for fixed values of scattering angles and incident neutrino energies as a function of the energy transferred to the nucleus.

angle and neutrino energy (hence not flux-folded) as a function of the lepton kinetic energy  $T_l$ , a measured quantity. The role of the different charged lepton masses appears not only in the trivial relative shift between the  $\nu_e$  and  $\nu_\mu$  CC cross sections, according to the identities

$$T_l = E_l - m_{\text{lepton}} = E_\nu - \omega - m_{\text{lepton}} = \omega_{\text{max}} - \omega, \quad (4)$$

but also in the strength and in the shape of the cross sections. In order to better illustrate these differences, we plot in the following figures (Figs. 6, 7 and 9) the differential cross sections not as a function of the lepton kinetic energy but as a function of the energy transfer  $\omega = E_\nu - m_{\text{lepton}} - T_l$ .

We start with the CRPA case which allows a simultaneous treatment of giant resonances and quasielastic excitations. In Fig. 6, we display the double-differential cross sections for different values of incoming neutrino energy and lepton scattering angle, both for  $\nu_e$  and  $\nu_\mu$ . In most cases the  $\nu_e$  and  $\nu_\mu$  results are quite similar, sometimes practically indistinguishable.

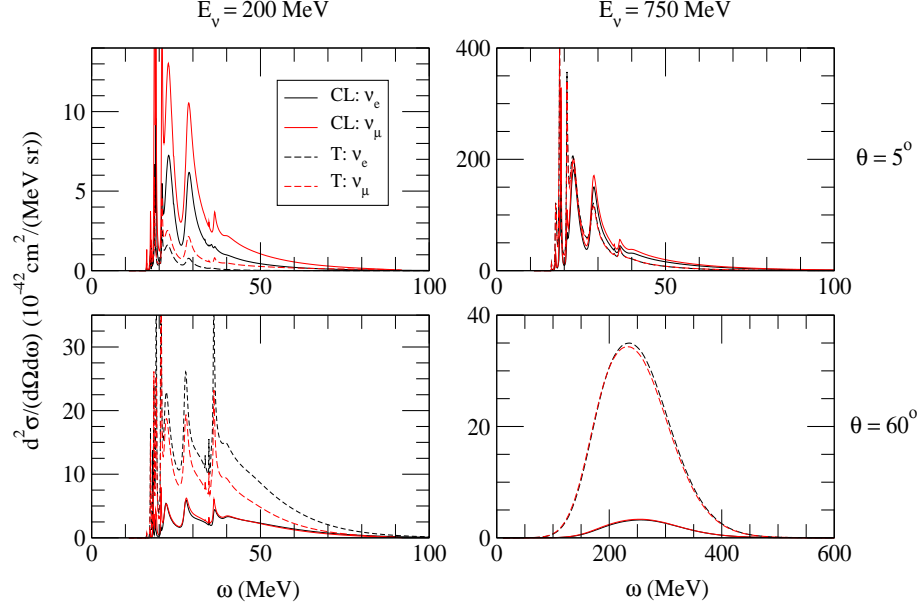


FIG. 7: (Color online) Coulomb-longitudinal (CL) and transverse (T) contributions to electron- and muon-neutrino CC double differential cross section on Carbon calculated in the CRPA approach for incident neutrino energies of 200 MeV and 750 MeV and two fixed values of scattering angles as a function of the transferred energy to the nucleus.

However, in some cases interesting differences appear. The first one is a consequence of the stringent limit on the maximum transferred energy  $\omega_{max} = E_\nu - m_{lepton}$  which has smaller values in the muon case. This threshold effect can be observed in Fig. 6 for  $E_\nu=150$  MeV and for  $E_\nu=200$  MeV in the case of 60 degrees. Other differences can be appreciated by observing the evolution with the scattering angle of the cross sections at small neutrino energies such as  $E_\nu=150$  MeV or  $E_\nu=200$  MeV. For small scattering angles such as 5 degrees,  $\nu_\mu$  cross sections are higher than the  $\nu_e$  ones, while for larger scattering angles, for example 60 degrees this behaviour is opposite. At intermediate angles the two cross sections are closer to each other. This angular behavior weakly survives at  $E_\nu=500$  MeV while for  $E_\nu=750$  MeV the  $\nu_e$  and  $\nu_\mu$  cross sections practically coincide for all the scattering angles.

It is also interesting to illustrate the behavior of  $\nu_e$  and  $\nu_\mu$  cross sections by separating their contribution, as shown in Fig.7 for incoming neutrino energies of  $E_\nu=200$  MeV and  $E_\nu=750$  MeV. According to the notation of Ref. [41], the global contribution related to the Coulomb and longitudinal multipole excitation operators (containing vector and axial com-

ponents) is labeled as CL. In the language of Refs. [20, 21] it represents the sum of isovector and isospin spin-longitudinal response contributions. The sum of transverse contributions, including the vector-axial interference term, is labeled as T. These are the terms containing the isospin spin-transverse response in the language of Refs. [20, 21]. As one can observe in Fig.7, for  $E_\nu=200$  MeV and  $\theta=5$  degrees (and in general for very forward scattering) the neutrino cross section is dominated by the CL contribution while for larger angles, such as 60 degrees, the transverse contribution T is dominant. At larger energies the transverse part dominates everywhere except for very small scattering angles. At  $E_\nu=200$  MeV and  $\theta = 5$  degrees the dominant CL contribution to the cross sections, as well as the smaller T one, are larger for  $\nu_\mu$  than for  $\nu_e$ , hence the larger  $\nu_\mu$  cross sections for this case. The relative weight of CL and T contributions is the result of a subtle interplay between lepton kinematic factors and response functions. The competition for dominance of the cross section between both, is very sensitive to energy and momentum transfer. The surprising dominance of  $\nu_\mu$  over  $\nu_e$  cross sections for small scattering angles is related to this and dictated by the non-trivial dependence of momentum transfer on lepton mass and scattering angle for forward scattering.

The non-trivial behaviour of the  $\nu_e$  cross sections with respect to the  $\nu_\mu$  ones is also illustrated in Fig. 8 where the ratio of the single differential cross section  $\frac{d\sigma_{\nu_e}}{d\cos\theta}/\frac{d\sigma_{\nu_\mu}}{d\cos\theta}$  is shown. For the 1p-1h channel in the CRPA approach, this ratio varies from  $\sim 1.5$  to 0.3 by increasing  $\cos\theta$  from 0 to 1 for a fixed neutrino of  $E_\nu=200$  MeV. At larger neutrino energies, such as  $E_\nu=750$  MeV, this ratio remains closer to 1 for the 1p-1h sector in CRPA. In Fig. 8 this quantity  $\frac{d\sigma_{\nu_e}}{d\cos\theta}/\frac{d\sigma_{\nu_\mu}}{d\cos\theta}$  at  $E_\nu=750$  MeV is given also for two other channels, the pion production and multinucleon excitations. For these channels we restrict the  $\nu_e/\nu_\mu$  comparison to the Martini *et al.* approach since they are not available in the Jachowicz *et al.* one. This  $\frac{d\sigma_{\nu_e}}{d\cos\theta}/\frac{d\sigma_{\nu_\mu}}{d\cos\theta}$  ratio, always larger than 1, is characterized by a smooth decreasing behavior. For the pion emission channel (via  $\Delta$  excitation) this ratio is larger than the one for the np-nh and 1p-1h excitations. For all the 3 channels the deviation from unity of the ratio is small at  $E_\nu=750$  MeV if compared to the  $E_\nu=200$  MeV 1p-1h CRPA result.

Concerning the pion production and multinucleon excitations, we display for completeness in Fig. 9 the  $\nu_e$  and  $\nu_\mu$  results obtained for these channels (as well as for the QE one) in the approach of Martini *et al.* for the double differential cross sections at incoming neutrino energies of  $E_\nu = 500$  MeV and  $E_\nu = 750$  MeV and scattering angles of 30 and 60

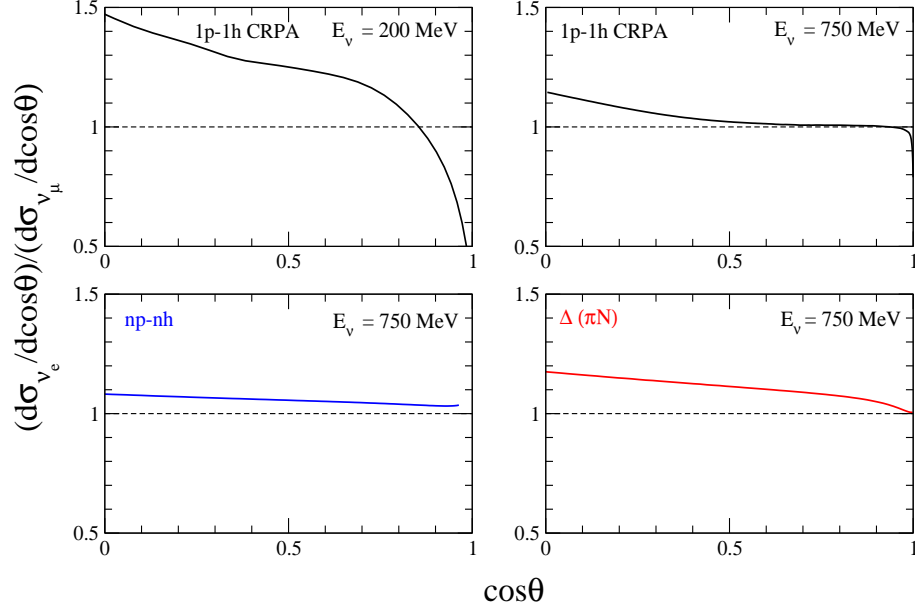


FIG. 8: (Color online) Ratio of the  $\nu_e$  over  $\nu_\mu$  differential cross section on Carbon calculated in the CRPA approach for two fixed values of incident neutrino energies as a function of the cosine of the lepton scattering angle. The 1p-1h results in the CRPA approach are shown for  $E_\nu=200$  MeV and  $E_\nu=750$  MeV. The np-nh excitations and the pion production (via  $\Delta$  excitation) results are shown for  $E_\nu=750$  MeV.

degrees. One observes the clear energy separation between the three channels, the highest energy transfer occurring for pion emission. Ignoring Fermi momentum and RPA reshaping effects, the quasi elastic peak occurs for an energy transfer  $\omega = Q^2/(2M_N)$  where  $Q^2 = q^2 - \omega^2 = 2E_\nu E_l(1 - \cos\theta) - m_l^2 + 2E_\nu(E_l - P_l)\cos\theta$ . In the electron case where  $m_l = 0$  it leads to  $\omega = E_\nu^2(1 - \cos\theta)/(M_N + E_\nu(1 - \cos\theta))$ . As for pion emission, in our model it occurs via  $\Delta$  excitation. In the same (nucleons at rest) approximation the pion emission peak is shifted towards large energy transfer, with the condition  $\omega = Q^2/(2M_N) + \Delta M$  with  $\Delta M = (M_\Delta^2 - M_N^2)/2M_N = 338$  MeV. This leads for  $\nu_e$  to  $\omega = (M_N\Delta M + E_\nu^2(1 - \cos\theta))/(M_N + E_\nu(1 - \cos\theta))$ . These formulas explain the positions of the quasielastic and  $\Delta$  peaks. As for the multinucleon excitations they lie between the two. The difference between the  $\nu_e$  and  $\nu_\mu$  cross sections mostly shows up in the energy transfer limit which is  $\omega_{max} \simeq E_\nu$  for electrons and  $\omega_{max} = E_\nu - m_\mu$  for muons. Hence it shows up mostly for pion production and it is more pronounced at low neutrino energies. It is also more pronounced

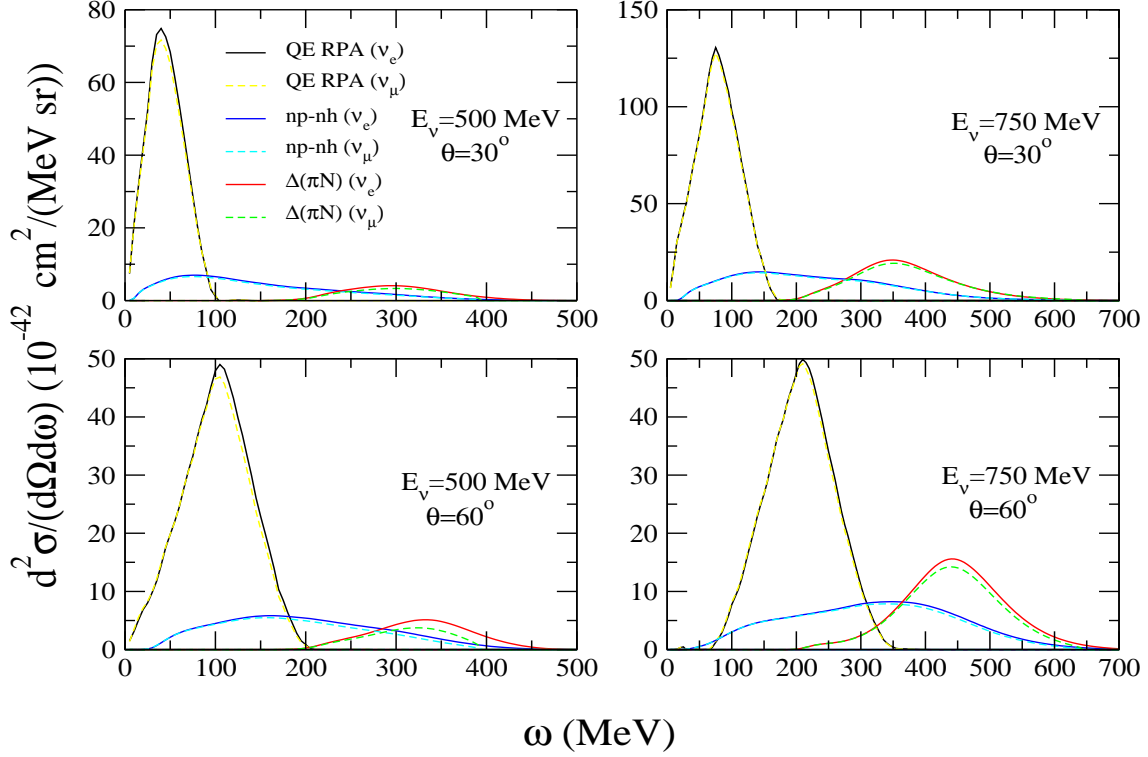


FIG. 9: (Color online) Electron- and muon-neutrino CC double differential cross section on Carbon calculated in the RPA approach for fixed values of scattering angles and incident neutrino energies as a function of the transferred energy to the nucleus. The genuine quasielastic (QE), multinucleon (np-nh), and incoherent one-pion production excitations are plotted separately.

at large scattering angles since the double differential cross sections move towards larger  $\omega$  when the scattering angle increases. This behavior with the scattering angle appears also in the previous Fig. 8.

#### IV. COMPARISON WITH THE T2K $\nu_e$ INCLUSIVE CROSS SECTIONS

The T2K collaboration published the first results for  $\nu_e$  charged-current inclusive differential cross sections on Carbon [37]. In this section we compare these experimental results with our predictions, restricting to the Martini *et al.* [20] RPA approach. We compute the  $\nu_e$  T2K flux averaged differential cross sections  $\frac{d\sigma}{dp_e}$  and  $\frac{d\sigma}{d\cos\theta_e}$  in the different excitation channels, namely quasielastic, multinucleon excitations (np-nh) and one-pion (coherent and incoherent) production. In Figs. 10 and 11 we plot the different exclusive channel contribu-

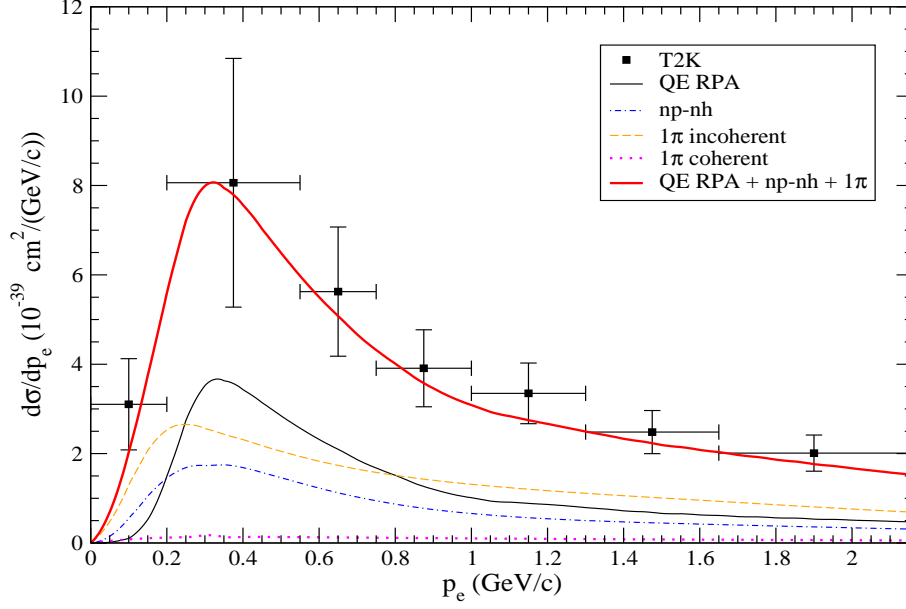


FIG. 10: (color online). T2K flux-integrated inclusive  $\nu_e$  CC differential cross section on Carbon per nucleon as a function of the electron momentum. The different contributions to this inclusive cross section obtained in the model of Ref. [20] are shown. The experimental T2K points are taken from Ref. [37].

tions separately, as well as their sum. This sum is in a good agreement with the experiment. Notice that this agreement needs the presence of the np-nh contribution (which even dominates the genuine QE one for small  $p_e$  values,  $p_e \lesssim 0.2$  GeV), a conclusion already reached by Martini and Ericson [31] in connection with the T2K inclusive  $\nu_\mu$  double differential cross sections [9]. This agreement with both  $\nu_\mu$  and  $\nu_e$  CC inclusive T2K flux folded differential cross sections is not systematically obtained in other approaches. For instance the SuSAv2 model by Ivanov *et al.* [51] reproduces well the CC inclusive T2K flux folded  $\nu_\mu$  double differential cross section but underestimates the CC inclusive T2K flux folded  $\nu_e$  single differential cross section. A comparison with these quantities has also been performed by Meucci and Giusti using the Relativistic Green's function model which turned to underestimate the  $\nu_\mu$  and  $\nu_e$  CC inclusive T2K data [52].

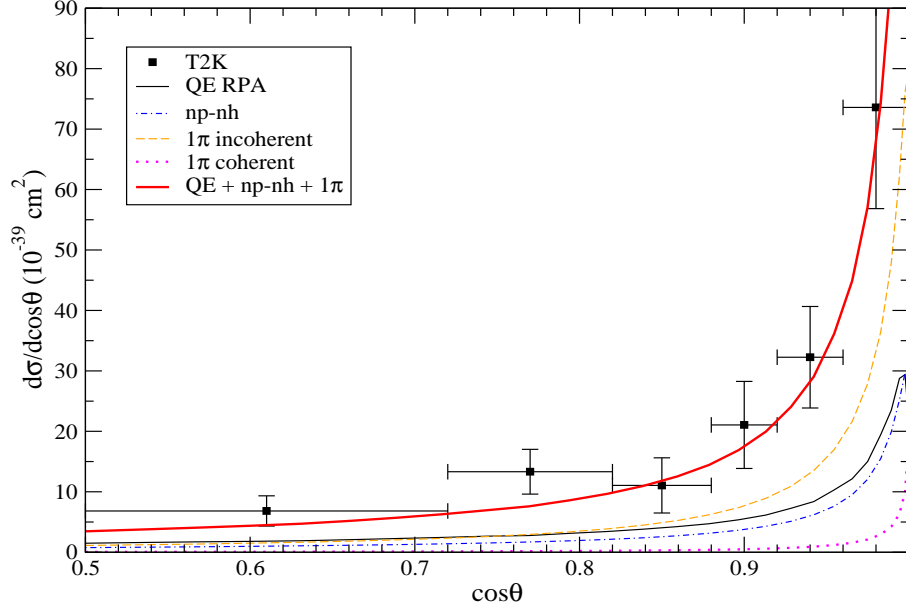


FIG. 11: (color online). T2K flux-integrated inclusive  $\nu_e$  CC differential cross section on Carbon per nucleon as a function of the cosine of the lepton scattering angle. The different contributions to this inclusive cross section obtained in the model of Ref. [20] are shown. The experimental T2K points are taken from Ref. [37].

## V. SUMMARY AND CONCLUSIONS

In conclusion, our study has dealt with several facets of the neutrino interaction with nuclei. A large part is devoted to the comparison between two different approaches to describe the interaction of neutrinos with nuclei. Both go beyond the impulse approximation and take into account, albeit in different ways, the interaction between nucleons. The CRPA approach of Jachowicz *et al.* starts from a continuum Hartree Fock description with Skyrme type interactions. The shell structure of the nucleus is present in this approach. The RPA-based approach of Martini *et al.* instead starts from a semiclassical description of the bare polarization propagator with a realistic nuclear density distribution. The shell structure is ignored in this description. The RPA effects also differ in the two approaches. For the residual interaction the first method uses the same Skyrme interaction as for the mean field, while in the approach of Martini *et al.*, it is parametrized in terms of pion and rho exchange and a contact Landau Migdal interaction. But the main difference is the possibility of mixing of  $\Delta$ -hole states in the second approach. It produces a general quenching of the

responses which shows up in most kinematical conditions that we have explored. The CRPA of Jachowicz *et al.* allows a description of giant resonances and quasielastic excitations while the RPA evaluations of Martini *et al.* includes quasielastic but also coherent and incoherent pion production, and multinucleon excitations.

We have compared the two approaches for the one nucleon - one hole excitations finding a reasonable agreement between them in the quasielastic peak region, with a trend for the RPA approach to lead to lower cross sections than the CRPA presumably due to the mixing with  $\Delta$  excitations. Other general trends are related to the more important high transferred-energy tail in the CRPA results and to a relative shift of the cross sections of  $\omega \simeq 18$  MeV, reflecting the presence of the nucleon separation energy in the CRPA calculations. The most striking difference is the appearance of giant resonance peaks in the CRPA results. The comparison of the two approaches has been performed for fixed values of the incoming neutrino energy as well as for the  $\nu_e$  T2K and MiniBooNE flux-folded cross sections.

We have also compared the  $\nu_e$  cross sections with the corresponding  $\nu_\mu$  ones for fixed values of the neutrino energy in order to investigate the impact of different charged lepton masses. We have found some non trivial behaviour, in particular for the 1p-1h excitations at low neutrino energies, such as an inversion with the scattering angle of the relative strength of  $\nu_e$  and  $\nu_\mu$  cross sections. Due to the different kinematical limits, the  $\nu_e$  cross sections are in general expected to be larger than the  $\nu_\mu$  ones, however for forward scattering angles this hierarchy is opposite. In the precision era of neutrino oscillation physics the  $\nu_e$  cross sections should be known with the same accuracy as the  $\nu_\mu$  ones. Trying to deduce the  $\nu_e$  cross sections from the experimental  $\nu_\mu$  ones can be considered only as a first approximation in the study of the  $\nu_e$  interactions.

Concerning the comparison with experiment, we have considered the inclusive  $\nu_e$  T2K flux-folded single-differential cross sections on Carbon and we have compared the data with the RPA-based approach. We have found a good agreement by adding the genuine quasielastic, the multinucleon and the one-pion production channels. This success obtained with a new flux, such as the  $\nu_e$  T2K one, complements those already reached with the three different fluxes, such as the MiniBooNE  $\nu_\mu$  and  $\bar{\nu}_\mu$ , and T2K  $\nu_\mu$  ones.



## Acknowledgments

This work was supported by the Interuniversity Attraction Poles Programme initiated by the Belgian Science Policy Office (BriX network P7/12) and by the Research Foundation Flanders (FWO-Flanders). M.M acknowledges also the support and the framework of the “Espace de Structure et de réactions Nucléaire Théorique” (ESNT, <http://esnt.cea.fr>) at CEA. We thank Raúl González-Jiménez, Carlotta Giusti and Andrea Meucci for useful discussions.

- 
- [1] A. A. Aguilar-Arevalo *et al.* [ MiniBooNE Collaboration ], Phys. Rev. **D81**, 092005 (2010).
  - [2] A. A. Aguilar-Arevalo *et al.* [MiniBooNE Collaboration], Phys. Rev. D **81**, 013005 (2010).
  - [3] A. A. Aguilar-Arevalo *et al.* [ MiniBooNE Collaboration ], Phys. Rev. **D82**, 092005 (2010).
  - [4] Y. Nakajima *et al.* [SciBooNE Collaboration], Phys. Rev. D **83**, 012005 (2011).
  - [5] A. A. Aguilar-Arevalo *et al.* [MiniBooNE Collaboration], Phys. Rev. D **83**, 052007 (2011).
  - [6] A. A. Aguilar-Arevalo *et al.* [MiniBooNE Collaboration], Phys. Rev. D **83**, 052009 (2011).
  - [7] C. Anderson *et al.* [ArgoNeuT Collaboration], Phys. Rev. Lett. **108**, 161802 (2012).
  - [8] A. A. Aguilar-Arevalo *et al.* [MiniBooNE Collaboration], Phys. Rev. D **88**, 032001 (2013).
  - [9] K. Abe *et al.* [T2K Collaboration], Phys. Rev. D **87**, 092003 (2013).
  - [10] G. A. Fiorentini *et al.* [MINERvA Collaboration], Phys. Rev. Lett. **111**, 022502 (2013).
  - [11] L. Fields *et al.* [MINERvA Collaboration], Phys. Rev. Lett. **111**, no. 2, 022501 (2013).
  - [12] R. Acciarri *et al.* [ArgoNeuT Collaboration], Phys. Rev. D **89**, no. 11, 112003 (2014).
  - [13] K. Abe *et al.* [T2K Collaboration], Phys. Rev. D **90**, no. 5, 052010 (2014).
  - [14] A. Higuera *et al.* [MINERvA Collaboration], Phys. Rev. Lett. **113**, no. 26, 261802 (2014).
  - [15] B. Eberly *et al.* [MINERvA Collaboration], arXiv:1406.6415 [hep-ex].
  - [16] R. Acciarri *et al.* [ArgoNeuT Collaboration], Phys. Rev. Lett. **113**, no. 26, 261801 (2014)  
[Erratum-ibid. **114**, no. 3, 039901 (2015)].
  - [17] T. Walton *et al.* [MINERvA Collaboration], Phys. Rev. D **91**, no. 7, 071301 (2015).
  - [18] T. Le *et al.* [for the MINERvA Collaboration], Phys. Lett. B **749**, 130 (2015).
  - [19] K. Abe *et al.* [T2K Collaboration], Phys. Rev. D **91**, no. 11, 112002 (2015)
  - [20] M. Martini, M. Ericson, G. Chanfray, J. Marteau, Phys. Rev. **C80**, 065501 (2009).

- [21] M. Martini, M. Ericson, G. Chanfray, J. Marteau, Phys. Rev. **C81**, 045502 (2010).
- [22] J. E. Amaro *et al.*, Phys. Lett. **B696**, 151-155 (2011).
- [23] J. Nieves, I. Ruiz Simo, M. J. Vicente Vacas, Phys. Rev. **C83**, 045501 (2011).
- [24] A. Bodek, H. Budd, M. E. Christy, Eur. Phys. J. **C71**, 1726 (2011).
- [25] M. Martini, M. Ericson and G. Chanfray, Phys. Rev. C **84**, 055502 (2011).
- [26] J. Nieves, I. Ruiz Simo and M. J. Vicente Vacas, Phys. Lett. B **707**, 72 (2012).
- [27] J. E. Amaro *et al.*, Phys. Rev. Lett. **108**, 152501 (2012).
- [28] O. Lalakulich, K. Gallmeister and U. Mosel, Phys. Rev. C **86**, 014614 (2012).
- [29] J. Nieves, I. Ruiz Simo and M. J. Vicente Vacas, Phys. Lett. B **721**, 90 (2013).
- [30] M. Martini and M. Ericson, Phys. Rev. C **87**, 065501 (2013).
- [31] M. Martini and M. Ericson, Phys. Rev. C **90**, 025501 (2014).
- [32] G. D. Megias *et al.*, Phys. Rev. D **91**, no. 7, 073004 (2015).
- [33] M. Ericson and M. Martini, Phys. Rev. C **91**, no. 3, 035501 (2015).
- [34] J. T. Sobczyk and J. Zmuda, Phys. Rev. C **91**, no. 4, 045501 (2015).
- [35] U. Mosel, Phys. Rev. C **91**, no. 6, 065501 (2015).
- [36] J. Blietschau *et al.* [Gargamelle Collaboration], Nucl. Phys. B **133**, 205 (1978).
- [37] K. Abe *et al.* [T2K Collaboration], Phys. Rev. Lett. **113**, 241803 (2014).
- [38] J. Wolcott *et al.* [MINERvA Collaboration], arXiv:1509.05729 [hep-ex].
- [39] M. Day and K. S. McFarland, Phys. Rev. D **86**, 053003 (2012).
- [40] N. Jachowicz, K. Heyde, J. Ryckebusch and S. Rombouts, Phys. Rev. C **65**, 025501 (2002).
- [41] V. Pandey, N. Jachowicz, J. Ryckebusch, T. Van Cuyck and W. Cosyn, Phys. Rev. C **89**, 024601 (2014).
- [42] V. Pandey, N. Jachowicz, T. Van Cuyck, J. Ryckebusch and M. Martini, Phys. Rev. C **92**, no. 2, 024606 (2015).
- [43] G. Chanfray and P. Schuck, Phys. Rev. A **38**, 4832 (1988).
- [44] W. M. Alberico, G. Chanfray, J. Delorme, M. Ericson and A. Molinari, Nucl. Phys. A **634**, 233 (1998).
- [45] H. De Vries, C. W. De Jager and C. De Vries, Atom. Data Nucl. Data Tabl. **36** 495 (1987).
- [46] W. M. Alberico, M. Ericson and A. Molinari, Nucl. Phys. A **379**, 429 (1982).
- [47] M. Ericson and T. E. O. Ericson, Annals Phys. **36**, 323 (1966).
- [48] J. Nieves, J. E. Amaro and M. Valverde, Phys. Rev. C **70**, 055503 (2004) [Phys. Rev. C **72**,

- 019902 (2005)].
- [49] K. Abe *et al.* [T2K Collaboration], Phys. Rev. D **87**, 012001 (2013).
  - [50] A. A. Aguilar-Arevalo *et al.* [MiniBooNE Collaboration], Phys. Rev. D **79**, 072002 (2009).
  - [51] M. V. Ivanov, G. D. Megias, R. Gonzalez-Jimenez, O. Moreno, M. B. Barbaro, J. A. Caballero and T. W. Donnelly, arXiv:1506.00801 [nucl-th].
  - [52] A. Meucci and C. Giusti, Phys. Rev. D **91**, no. 9, 093004 (2015).